Functionally Graded Lattices in Additively Manufactured Rib Implants Result in Similar Biomechanics

Richa Gupta[1]
Lauren Judkins[2]
Chet S. Friday[1]
Joseph B. Ulsh[1]
Stephen Kovach[1]
Samir Mehta[1]
Charles Tomonto[3]
Guha Manogharan[2]
Michael W. Hast[1]

1McKay Orthopaedic Research Lab
Department of Orthopaedic Surgery,
University of Pennsylvania,

2SHAPE Lab
Department of Mechanical and Nuclear Engineering, Pennsylvania State University

3Johnson and Johnson 3D Printing
Miami, FL

Introductions

Rib fractures are difficult to treat surgically due to large variability in bone size, curvature, and mechanical properties of the natural bone. Titanium alloy (Ti6Al4V) rib implants are used when open reduction internal fixation is required for reconstruction. Undesirable clinical outcomes such as chest tightness, component loosening, and secondary fracture at the ends of implants are often reported, with revision surgery required in up to 15% of patients.[1] Rib implants may be improved with 3D printing or additive manufacturing (AM), because this process allows for creation of patient-specific geometries and tuning of mechanical properties of implants. In a previous study, we printed 100 x 10 x 1.5 mm Ti6Al4V beams, and decreased bending stiffness up to 15% by uniformly changing the internal lattice structure.[2] Decreasing the mechanical stiffness towards the ends of rib implants may reduce incidence of secondary fracture, but interfragmentary fixation strength cannot be compromised. In the current study, we sought to characterize the biomechanics of functionally graded lattice designs by testing implants in a biofidelic synthetic bone model. We hypothesized that, by making gradient-based changes in internal lattice architecture, we could maintain requisite construct rigidity at the fracture line and decrease the likelihood of secondary fracture at implant ends.

Methods

This study included 6 implant designs (n = 6), with 5 custom AM implants, and a traditionally manufactured titanium control group (MatrixRib, DePuy Synthes, Figure 1A). Custom implants were manufactured with variable rectilinear infill patterns between the 0.5 mm floors and roofs of the plates. Groups included a sparse infill group, 3 functionally graded infill groups (Gradients 1, 2, and 3) and a solid infill group. Custom implants had a similar width (10 mm), thickness (1.5 mm), and length (70 mm) as control implants, but did not include notches to allow for maximization of infill volume. All custom implants were additively manufactured from Ti-6Al-4V powder via laser-powder bed fusion and heat-treated using standard processing conditions. Custom 4th generation Sawbones were designed and manufactured to represent a transverse fracture at the apex of curvature on a 50th percentile male's 4th rib on the left side. Components were implanted with six 2.7 mm diameter nonlocking cortical screws by fellowship-trained orthopaedic surgeons. To simulate post-operative respiration, ribs were compressed in a two-point bend test to generate flexural moments between 0 – 0.5 Nm at the fracture line. Tests were run at 3 Hz for 360,000 cycles to simulate 17.5 days of post-operative breathing (Figure 1B).[3] 3D motion capture was performed at 100 Hz to measure 6 degrees of freedom of interfragmentary motion during cyclic loading. Following cyclic testing, the plates were subjected to ramp-to-failure tests at a rate of 1 mm/s and failure mechanisms were recorded. Differences in cyclic stiffness, 3D interfragmentary motions, ramp-to-failure stiffness, maximum load, and work to failure were tested for significance using one-way ANOVA tests with post-hoc Holm-Sidak pairwise comparisons.

Results

During cyclic testing the Control group demonstrated significantly decreased construct stiffness, as measured by the load cell (0.76 ± 0.28 N/mm), compared to all AM implant designs (means between 1.35 – 1.61 N/mm) (Figure 2A). 3D motion capture indicated that the Control group bone fragments rotated significantly more about the bending axis (2.7 ± 1.3 deg) than the other

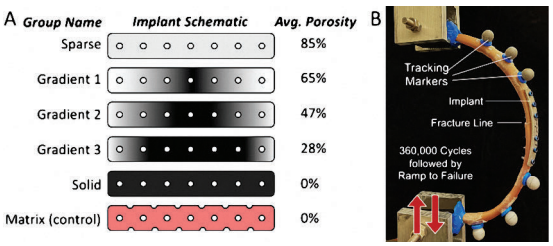

Figure 1. (A) Schematic diagram outlining the functionally graded implant designs tested in the experiment, along with average porosities of the infill for each design; **(B)** Photograph of a synthetic rib undergoing 2-point bend testing. 3D motion tracking markers were used to quantify interfragmentary motions.

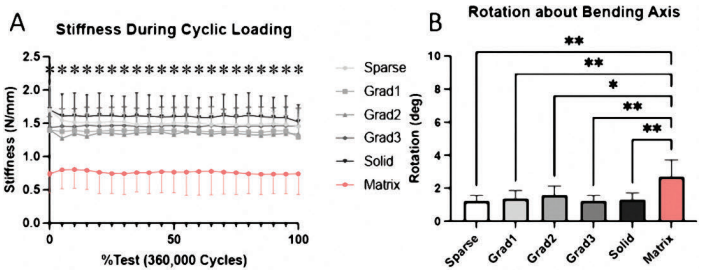

Figure 2. (A) Load-cell-measured stiffness throughout cyclic loading, with significant differences between the control (pink) and experimental (gray) groups. **(B)** Mean interfragmentary rotations about the bending axis during cyclic loading. * = $p < 0.05$; ** = $p < 0.001$.

groups (means between 1.2 – 1.6 deg) (Figure 2B). There were no significant differences between groups for the other 5 degrees of freedom. Ramp to failure testing showed that Control group bending stiffness (0.84 ± 0.28 N/mm) was significantly lower than the stiffness of the Sparse group (1.40 ± 0.07 N/mm), but not other groups (Figure 3A). Ultimate force values were highest for the Gradient 2 group (35.8 ± 5.6 N, which was significantly different from the Gradient 1 (25.8 ± 4.2 N) and Control (25.9 ± 2.7 N) groups (Figure 3B). There were no significant differences between groups for work prior to failure. All constructs failed via bone fracture at the most posterior screw hole.

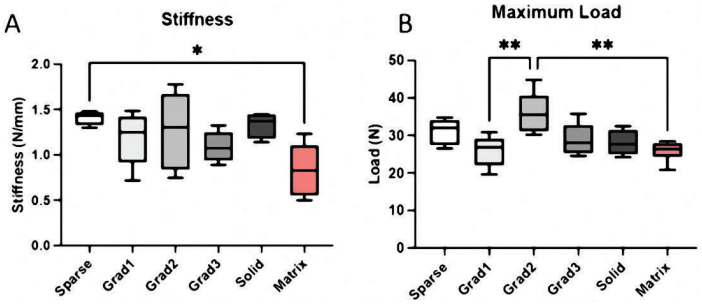

Figure 2. (A) Load-cell-measured stiffness throughout cyclic loading, with significant differences between the control (pink) and experimental (gray) groups. **(B)** Mean interfragmentary rotations about the bending axis during cyclic loading. * = $p < 0.05$; ** = $p < 0.001$.

Discussion

Results from this study only prove a portion our initial hypothesis. Using Control implant behavior as a gold-standard, our implant designs were largely successful in controlling interfragmentary motion and showed no signs of permanent deformation during the cyclic load test. The lack of notches in AM designs likely caused increased resistance to bending. Interestingly, changes in functionally graded lattice architecture did not lead to many significant differences in AM implant performance throughout the experiment. Our designs did not result in predictable stepwise changes to stiffness or maximum load, and functional grading of the lattice did not change the failure mechanism, which was the same for all test specimens. These results are likely confounded by the thin cross-sectional area of the implants and small volume of bone available for screw purchase. Additional studies are ongoing to map changes in mechanical behavior of functionally graded implants.

Significance/Clinical Relevance

Additive manufactured orthopaedic implants may benefit from the use of functionally graded lattice structures. In the case of rib implants, it is likely that the screw hole—not implant stiffness—creates the stress riser responsible for secondary fractures at implant ends.

Acknowledgements

This study was supported by the Manufacturing Pennsylvania Innovation Program and NIH/NIAMS P30AR069619. DePuy Synthes provided materials and technical support.

References

1. Lafferty P, Anavian J, Will R, *et al* Operative treatment of chest wall injuries: indications, technique, and outcomes. *JBJS A*, 2011; 5;93(1):97-110.

2. Judkins L, Jupta R, Gabriele C, *et al.* On Additive Manufacturing of Rib Fracture Fixation Implants: The Role of Lattice Design. *ASME IMECE*, 2021.

3. Fitzpatrick D, Denard P, Phelan D , *et al.* Operative stabilization of flail chest injuries: review of literature and fixation options. *Eur J Trauma Emerg Surg*, 2010.